CONTINUOUS SEPARATION OF WATER-OIL MIXTURE

USING SURFACE MODIFIED MEMBRANES

by

Tianhan Jiang

B.S. in Chemical Engineering, Hebei University of Technology, 2010

Submitted to the Graduate Faculty of

Swanson School of Engineering in partial fulfillment

of the requirements for the degree of

Master of Science

University of Pittsburgh

2012

UNIVERSITY OF PITTSBURGH

SWANSON SCHOOL OF ENGINEERING

This thesis was presented

by

Tianhan Jiang

It was defended on

April 6, 2012

and approved by

Sachin Velankar, PhD, Associate Professor,
Department of Chemical and Petroleum Engineering

Lei Li, PhD, Assistant Professor,
Department of Chemical and Petroleum Engineering

Di Gao, PhD, Associate Professor,
Department of Chemical and Petroleum Engineering
Thesis Advisor

CONTINUOUS SEPARATION OF WATER-OIL MIXTURE

USING SURFACE MODIFIED MEMBRANES

Tianhan Jiang, M.S.

University of Pittsburgh, 2012

In this study, the surfaces of membranes are modified with custom-designed polymers for separation of water-oil mixture. By tuning the chemical structure of the polymers, the water and oil repellencies of the membrane can be tailored. In particular, two types of membranes have been made and used to construct a continuous water-oil separator: one allows oil to pass but stops water, and the other allows water to pass but stops oil. The continuous water-oil separator splits one stream of water-oil mixture into two streams: a water stream that has less than 0.075 wt% of oil, and an oil stream that has less than 0.01 wt% of water.

Because of the surface texture of the membranes, the modified membranes possess extreme repellencies to either water or oil while can be completely wetted by the other liquid. The two types of membranes used in the water-oil separator are (i) superhydrophilic but superoleophobic (denote as HBO) and (ii) superoleophilic but superhydrphobic (denote as OBH). The super hydro/oleo-philicity and hydro/oleo-phobicity are characterized and explained by Wenzel and Cassie-Baxter models. In addition, the robustness of the hydro/oleo-philic and hydro/oleo-phobic states is analyzed, and critical parameters that affect the robustness of these states are determined.

The performance of the membranes during the separation of water-oil mixture is characterized by measuring (i) the relationship between pressure and volume flux, (ii) break-down pressure, (iii) break-down time, and (iv) the oil (water) percentage in the water (oil) stream after separation. These parameters provide guidance to the design and operation of the continuous water-oil separator.

TABLE OF CONTENTS

LIST OF TABLE

LIST OF FIGURES

NOMENCLATURE

Superhydrophilic: a behavior of a solid surface, which has a water contact angle almost equal to 0^o.

Superhydrophobic: a behavior of a solid surface, which has a water contact angle greater than 150^o.

Superoleophilic: a behavior of a solid surface, which has contact angle with organic liquids almost equal to 0^o.

Superoleophobic: a behavior of a solid surface, which has contact angle with organic liquids greater than 150^o.

Substrates: the word "substrates" in this thesis represents the material that is prepared for the coating process afterward.

Membranes: the word "membranes" in this thesis represents the polymer-modified substrates which already have desired characteristics (say, superhydrophilic but superoleophobic), even if the coating process and certain characteristics are not mentioned in the sentence.

HBO Membranes: referring to superhydrophilic but superoleophobic membranes which allow only water to flow through and blocking oil.

OBH Membranes: referring to superoleophilic but superhydrophobic membranes which allow only oil to flow through and blocking water.

HBO Polymer: referring to the custom-designed polymer (in this work fluoroalkyl phosphates) dip-coating on substrates and make them become superhydrophilic but superoleophobic membranes (HBO membranes). Such polymer usually contains at least one hydrophilic section (typically groups that possess positive or negative charges in an aqueous

solution) and one oleophobic section (typically fluorocarbon groups).

OBH Polymer: referring to the custom-designed polymer (in this work fluorinated trimethoxysilane and fluorinated trichlorosilane) dip-coating on substrates and make them become superoleophilic but superhydophobic membranes (OBH membranes).

ACKNOWLEDGEMENT

I would like to express my sincere gratitude to my advisor, Professor Di Gao. This thesis would not have been possible without his support and patiently advice throughout my research and thesis writing. With his enthusiasm, his inspiration, and immense knowledge, he helped me to overcome all difficulties.

I would like to express my appreciation to my committee members, Professor Sachin S. Velankar and Professor Lei Li, for the insightful comments and advices.

My sincere thanks also go to my group members, Jiamin Wu and Dr. Mengnan Qu, for the guidance and assistance with their strong experimental skills, and to the rest of my group members, Umang Desai, Dr. Chengkun Xu, Guangyu Lv, IInk Pattarapa, and Jason Lee, for their inspiring comments in the discussion.

I would like to dedicate this thesis to my wonderful parents and express my deepest appreciation for always stand by my side and support me both spiritually and financially. They have waited this moment for so long and given so much, this thesis will be a start of reward. This thesis is also dedicated to my girlfriend, Yan Gao, who gave me support and encouragement throughout the last five years.

1.0 INTRODUCTION

1.1 MOTIVATION

Previous members of my research group have developed methods of fabricating surfaces with extreme wettability or repellency to liquid (such as water and oil) on various substrates by tailoring the surface topography and chemistry (Cao, 2010). One application is that if the surface of a fluid-permeable membrane can possess such extreme wettability or repellency to different liquids, it has the potential of allowing one type of liquid to pass while stops the others. In this work, two membranes are made: one allows oil to pass but stops water, and the other allows water to pass but stops oil. The mechanism of these membranes will be reviewed in later sections (1.4).

These two types of membranes are made and the performance of the membranes during the separation of water-oil mixture is characterized by measuring (i) the relationship between pressure and volume flux, (ii) break-down pressure, (iii) break-down time, and (iv) the oil (water) percentage in the water (oil) stream after separation. These parameters provide guidance to the design and operation of the continuous water-oil separator.

A lab-scale prototype of the continuous water-oil separator is designed and constructed. A detailed introduction of the separator is presented in Section 1.5, and the designing work is expanded in Chapter 5.0 .

1.2 CONVENTIONAL WATER-OIL SEPARATION METHODS

Continuality of the separation of the water-oil mixture is an important but challenging issue in the petroleum industry, environmental protection, and separation and purification processes of chemicals.

In petroleum industry, because of the uncertainty of the flow pattern of oil-water mixture, water content in crude oil may cause problem in transportation pipeline design, selection of pump, and potential equipment corrosion. In the downstream stages of oil production, water content may also arise problems, for example, deactivate catalysts. Therefore, water is generally separated before the transportation of oil. However, water-oil mixture was formed during the production stage of crude oil or even during the crude oil was in the reservoir formation (for example, mixture was formed when waterflooding is applied), and in most cases, water would appear as emulsion. These facts have increased the difficulties of water-oil separation. Gravity separation method has been widely used in water separation from crude oil (Rao & Patil, 1998). However, this method has relatively low efficiency which is becoming a problem due to the increasingly water content in crude oil (water content can be more than 90% in oil wells that have decades of production life).

Water-oil separators are often required by environmental protection organizations for water purification before discharge. For example, water-oil separator for separating oil from bilge water (called oily water separator) is required by MARPOL convention. The separators on ships are also gravity-based separator. The state-of-art industrialized separator is hydrocyclone water-oil separatorn (Belaidi & Thew, 2003). For example, liquid-liquid hydrocyclone water-oil separator, product of SIEMENS. Although this type of separation method has a very high efficiency and satisfactory purity after separation, but it is generally energy consuming.

Other separation methods, including electrically-enhanced phase separation (Taylor, 1996) and traditional membrane separation (Fernandez, Soria, Garcia-Tourn, & Izquierdo, 2001), are also used in industry sometimes. However, all of these methods have certain weaknesses, such as long residence time, high operating cost, and/or low separation efficiency.

The continuous water-oil separator we designed here can be an alternative separation method which is (i)highly efficient: due to the nature of continuous separation and the potential to be scaled up, (ii)cost effective: estimated cost of preparing the membrane is $\$0.2/ft^2$, and (iii)low energy consuming: can be operated under normal pressure (with pipeline pumps).

1.3 HYDROPHILICITY AND HYDROPHOBICITY

1.3.1 Contact Angle - Measurements of Surface Wettability

Wettability is the representation of the ability of a liquid to spread on a solid surface and is often measured by contact angle (θ). Figure 1 describes three different liquid having different wettability on the same solid surface.

Contact angle can be quantitatively described by Young's equation,

$$\gamma_{SG}=\gamma_{SL}+\gamma_{LG}\cos\theta \tag{1.1}$$

$\gamma_{SG},\gamma_{SL},\gamma_{LG}$ are the surface tension between solid phase and gas/vapor phase, solid phase and liquid phase, liquid phase and gas/vapor phase, respectively. (Young, 1805)

To describe the effect of surface roughness on contact angle, Wenzel state and Cassie–Baxter state are introduced in Section 1.4, and they will be used in Chapter 4 (4.1) to explain the observed wetting phenomena on polymer-modified membranes.

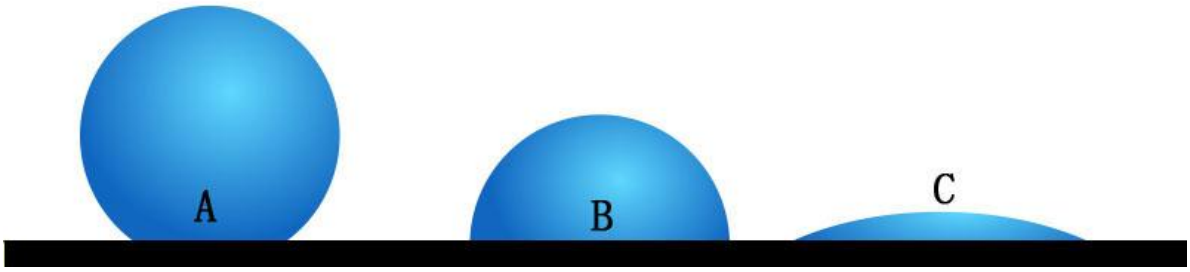

Figure 1 Different wettability of fluid A, B and C on the same solid surface S. Wettability relation: A<B<C.

1.4 WETTING ON ROUGH SURFACES

The effect of surface roughness on surface wettability has been explained by Wenzel and Cassie-Baxter models.

1.4.1 Wenzel State and Cassie-Baxter State

Wenzel model can be quantitatively represented by equation (1.2). (Wenzel, Resistance of solid surfaces to wetting by water, 1936)

θ_{flat} denotes the intrinsic contact angle, which is defined as the contact angle on an ideally flat surface, which possesses the same surface chemistry as the textured surface. When a liquid droplet is in intimate contact (no air trapped between the rough surface and the liquid) with a textured surface, the apparent contact angle θ_{rough} is determined by the Wenzel equation as

$$\cos\theta_{rough} = r\cos\theta_{flat} \tag{1.2}$$

$\cos\theta_{rough} = r\cos\theta_{flat}$, where r is the roughness factor defined as the ratio of the actual surface area to the projection surface area. Since r is always larger than 1 for any rough surface, this equation indicates that if $\theta_{flat} < 90°$ then $\theta_{rough} < \theta_{flat}$, and if $\theta_{flat} > 90°$ then $\theta_{rough} > \theta_{flat}$. In other words, the surface hydro/oleo-philicity or hydro/oleo-phobicity can be further enhanced by the surface roughness.

Since the substrates used in this work is woven or non-woven structure (for structure detail, see Section 4.1.2), Wenzel's model may be applicable to the surfaces. For example, a polymer-modified HBO surface is in fully contact with water (Figure 2, A).

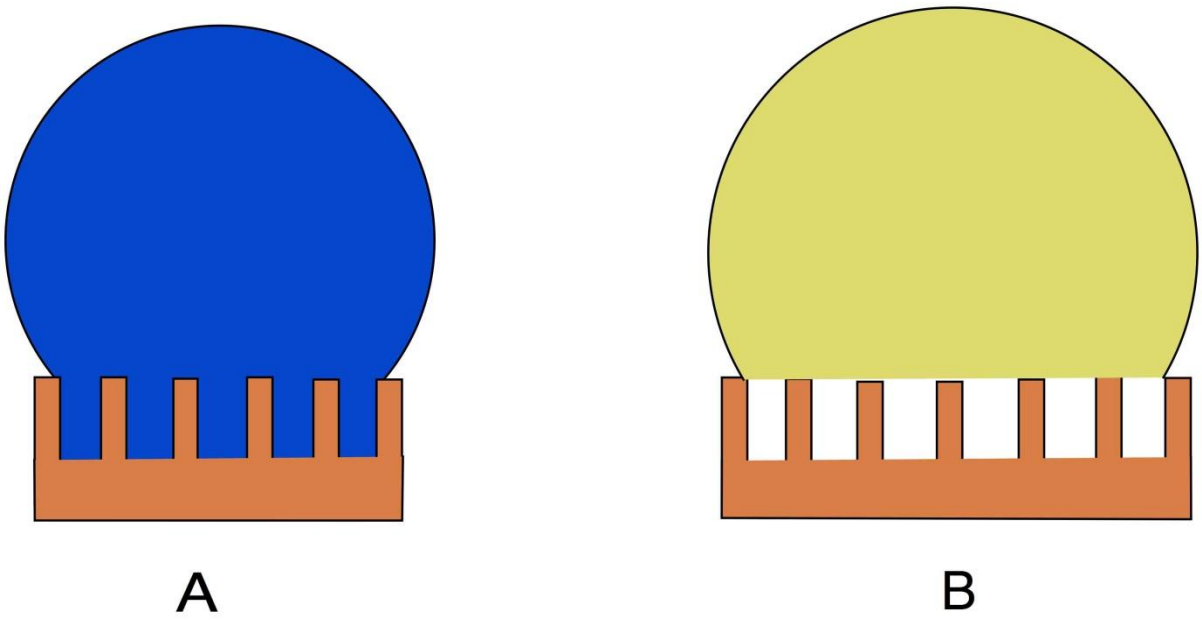

Figure 2 Scheme of Wenzel State (A) and Cassie-Baxter state (B).

In Cassie-Baxter state, the liquid droplet is thought to be in contact with a composite surface of solid and air (Figure 2, B).

The apparent contact angle θ_{rough} is determined by the Cassie-Baxter equation as

$$\cos\theta_{rough} = \varphi_s \cos\theta_{flat} + \varphi_v \cos\theta_{LV} \tag{1.3}$$

where φ_s is the area fraction of the solid in contact with the liquid, φ_v is the area fraction of the air in contact with the liquid, θ_{LV} is the contact angle of water on air, which will normally equals to $180°$ (Cassie & Baxter, 1944). After substitute $\cos\theta_{LV} = -1$ into equation (1.3), we get

$$\cos\theta_{rough} = \varphi_s \cos\theta_{flat} - (1-\varphi_s) \tag{1.4}$$

From equation (1.4), monotonic decrease of φ_s results in an increase of $\cos\theta_{rough}$, and eventually leads to a super-hydro/oleo-phobic state.

The minimal value of θ_{flat} in Wenzel state is apparently 0, with $\cos\theta_{flat}$=1. To find the maximum value of θ_{flat}, which is the conjoining point with Cassie-Baxter, equation (1.2) can be substituted into equation (1.4), and then we get

$$\cos\theta_c = -\frac{1-\varphi_s}{r-\varphi_s} \tag{1.5}$$

where $\cos\theta_c$ denotes the maximum value of $\cos\theta_{flat}$. When θ_{flat} is larger than the value of θ_c, Wenzel state is switched to Cassie-Baxter state.

1.4.2 Metastable Cassie-Baxter State

As previously reported (Cao, Hu, & Gao, 2007), some special topography on the material surface, e.g. “re-entrant” and “overhang” structure (shown in Figure 3 schematically), is considered as one of the reason that caused super-hydro/oleo-phobic. The re-entrant structure is widely adopted by other authors when explaining the super-hydro/oleo-phobic phenomena (Tuteja, Choi, Mabry, McKinley, & Cohen, Robust omniphobic surfaces, 2008) (Koishi, Yasuoka, Fujikawa, Ebisuzaki, & Zeng, 2009) (Varanasi, Deng, Hsu, & Bhate, 2009) (Boreyko, Baker, Poley, & Chen, 2011).

When a liquid is in contact with such surface texture, the capillary force may prevent the liquid from completely penetrating the pores of the surface texture once the local texture angle (ψ, ranging from $0°$ to $180°$ for the cylindrical features) is less than θ_{flat}, even if the θ_{flat} of the liquid may be much smaller than $90°$.

Re-entrant structure often but not necessarily leads to metastable Cassie-Baxter state, as a local minimum surface free energy is created by the unique structure. As illustrated in Figure 3, liquid is prevented from penetrate through the opening between two fibers within certain pressure. This pressure, is called break-down pressure macroscopically, will be discussed in detail in later chapters. Break-down pressure was determined for each polymer-coated membrane and used as a guide to design the separator and the operational conditions.

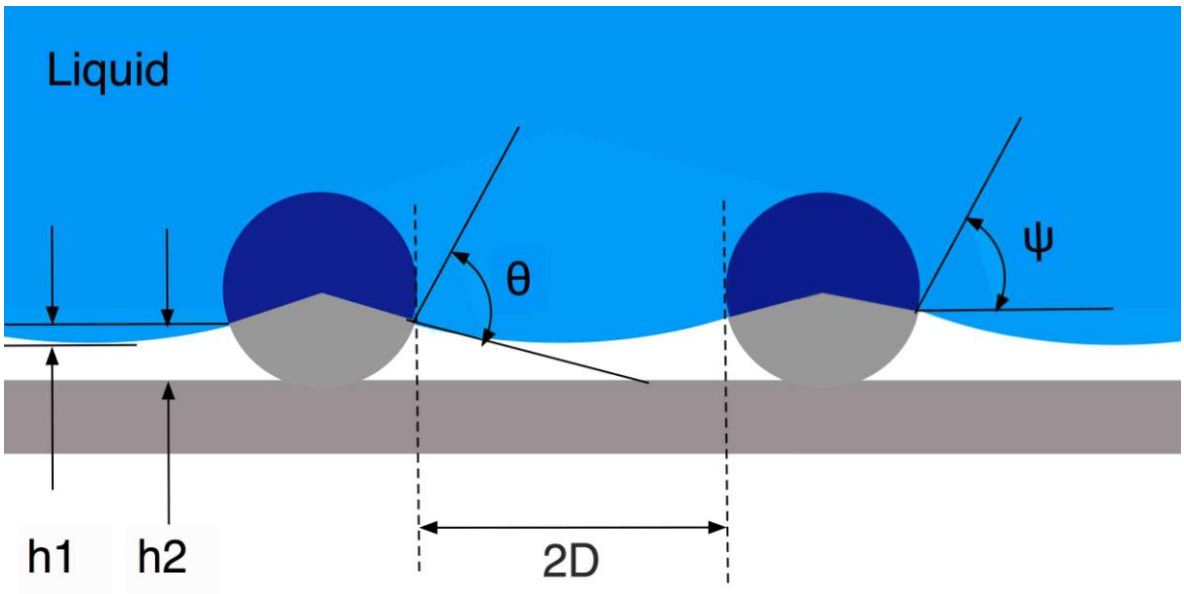

Figure 3 Scheme of local texture angle ψ and intrinsic contact angle θ between individual fibers.

To evaluate the robustness of the metastable Cassie-Baxter state, two parameters, the robustness height (H*) and the robustness angle (T*), have been adopted (Tuteja, Choi, Mabry, McKinley, & Cohen, Robust omniphobic surfaces, 2008). Through increasing the magnitude of the robustness parameters (H* and T*), the stability of the metastable composite interface can be improved. The parameter H*, arising from the ratio of the sagging height (h_1) and the maximum pore depth (h_2) (shown in Figure 3), is given as

$$H^* = (1-\cos\theta)R\ell_{cap}/D^2 \tag{1.6}$$

Where R is the fiber radius, $\ell_{cap} = \sqrt{\gamma_{lv}/\rho g}$ is the capillary length of the liquid, γ_{lv} is the liquid surface tension, ρ is the liquid density, g is the acceleration due to gravity, and D is the half of the inter-fiber gap.

The parameter T*, arising from the sagging angle of $\delta\theta = \theta - \psi_{\min}$, is given as

$$T^* = \ell_{cap}\sin(\theta-\psi_{\min})/(2D) \tag{1.7}$$

and the minimum local texture angle $\psi_{\min}$ used herein equals to 0.

The robustness parameters are determined by the liquid properties (θ and ℓ_{cap}) and the surface properties (R, D and $\psi_{\min}$).

1.5 SCHEME OF THE CONTINUOUS WATER-OIL SEPARATOR

The core part of the water-oil separator (Figure 4) includes a specially designed separation tube which has one inlet and two outlets: the oil outlet and the water outlet. When the water-oil mixture is fed continuously into the inlet at a certain flow rate, water and oil will flow out from the two outlets separately at a constant and controlled flow rate.

In this work, several parameters are determined in order to design a separation device with scale-up potential.

First, both HBO and OBH membranes only function when the pressure drop across the membrane is within a specific range. When the pressure drop is higher than a critical value, which is called break-down pressure, both water and oil will penetrate the membrane. One of the tasks is to determine the break-down pressure.

The second task is to determine the correlation between volume flux and pressure for each membrane within the operational pressure range.

The third task is to design and fabricate a water-oil separator based on the characterization of the membranes. As a demo, a lab-scale separator (Figure 5) is designed for water-hexadecane separation in this thesis in Chapter 5.0 . Additional monitoring and pumping devices will be introduced in Chapter 3.0 .

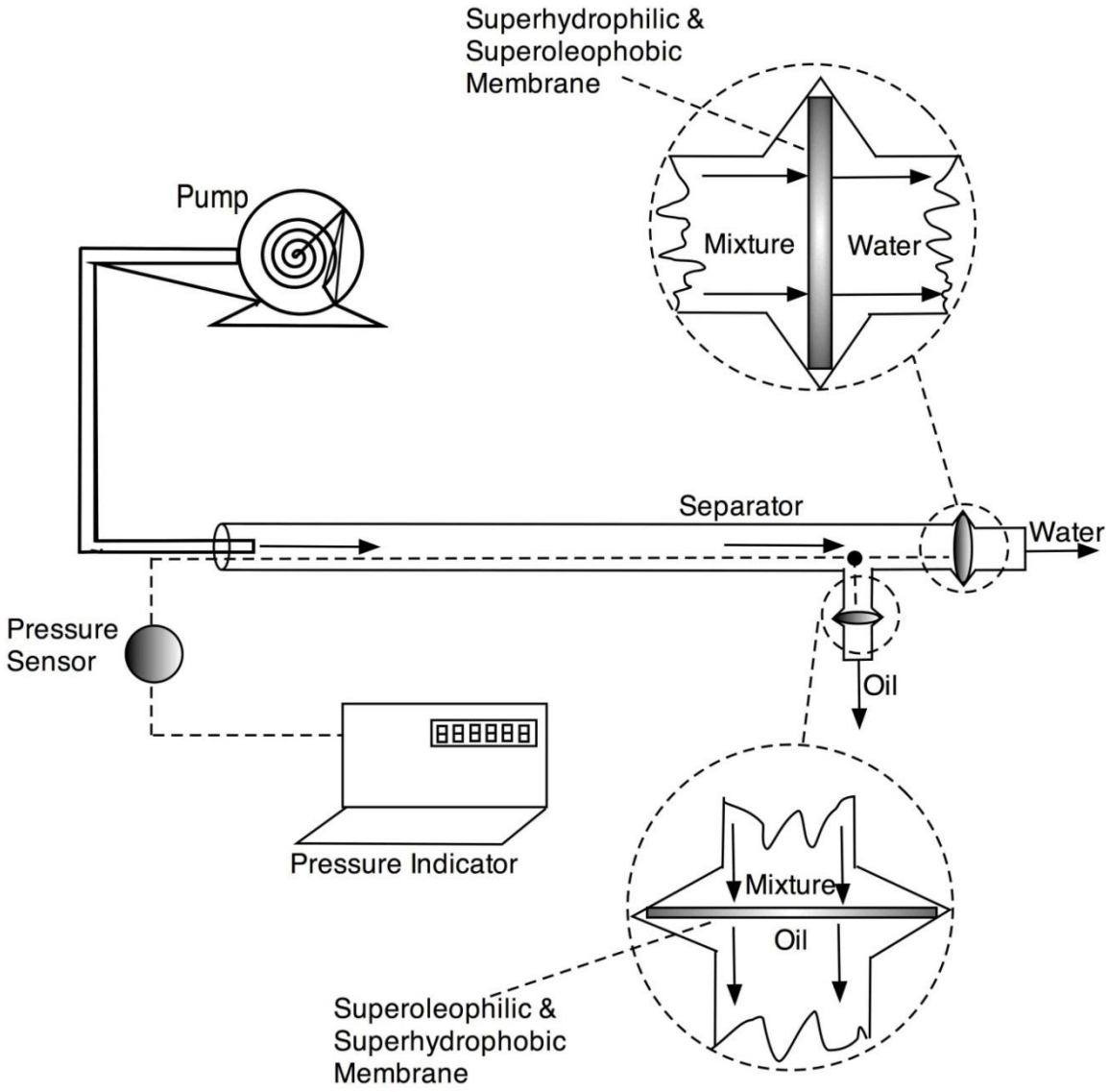

Figure 4 Scheme of water-oil separator.

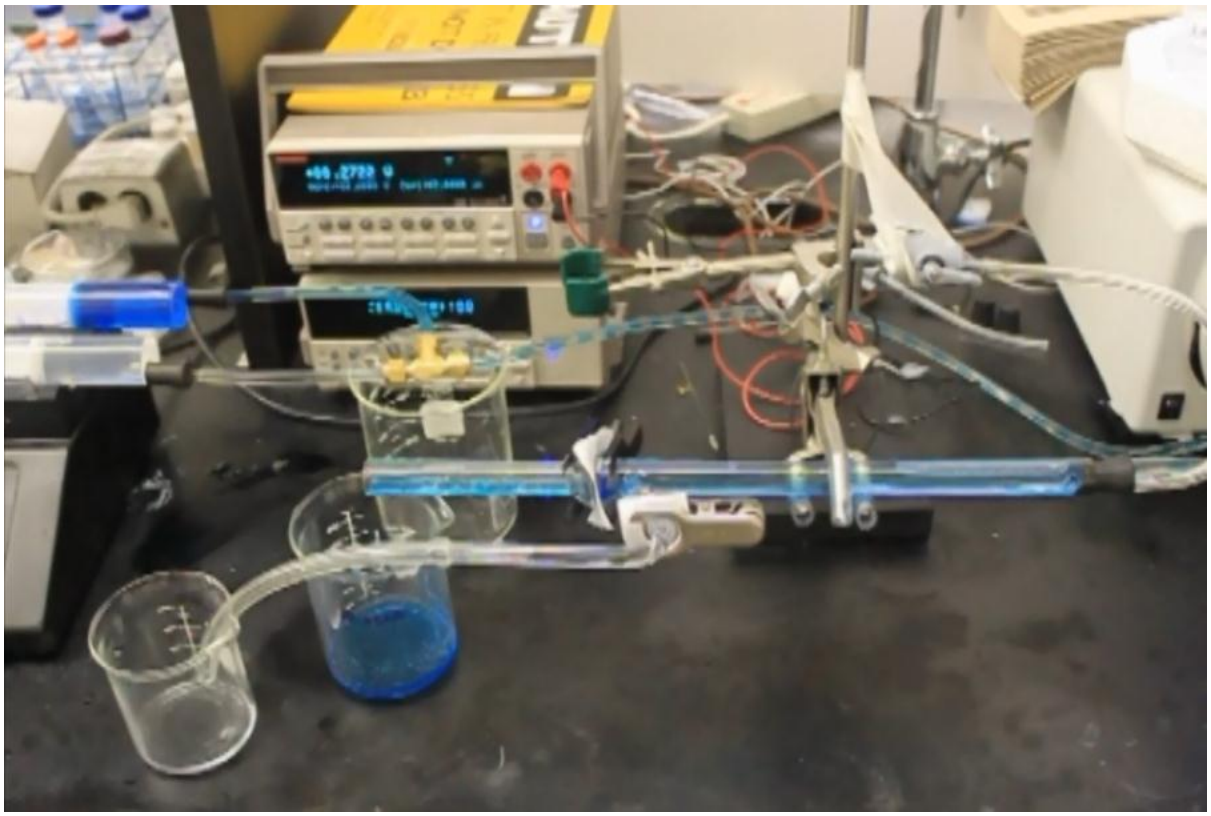

Figure 5 Continuous water-oil separator with pressure sensor and indicator.

2.0 SURFACE MODIFICATION PROCESS

2.1 COATING POLYMER CONCENTRATION OPTIMIZATION

Before the custom-designed polymer is used for coating HBO and OBH membranes, the concentration should be optimized. The effect of polymer concentration on contact angle is studied and the result is shown in Table 1. It is observed that among all the concentrations tested, 1:10 is the only concentration that makes the membrane superhydrophilic while maintaining a high oil contact angle (145.1^{o}).

Table 1 Effect of polymer concentration on contact angle

	1:10	1:20	1:40	1:70	1:100	Uncoated
Hexadecane	145.1^{o}	149.1^{o}	133.5^{o}	137.6^{o}	128.3^{o}	0^{o}
Water-30''	0^{o}	81.3^{o}	89.7^{o}	119.6^{o}	123.6^{o}	0^{o}
Water-2'	0^{o}	57.1^{o}	85.5^{o}	103.2^{o}	118.8^{o}	0^{o}
Water-4'	0^{o}	25.2^{o}	83.7^{o}	99.8^{o}	109.1^{o}	0^{o}
Water-7'	0^{o}	0^{o}	76.5^{o}	97.1^{o}	106.2^{o}	0^{o}

Note:

1:10 refers to the volume ratio of polymer to DI water.
Water-30'' and water-2' refer to the contact angle of water on the membrane at 30 sec and 2 min, respectively.

2.2 COATING PROCESS

Three substrates, cotton fabrics, glass fiber membranes and polyester (PET) membranes, are tested. All of the substrates are dip-coated with custom-designed HBO polymer and OBH polymer. To evaluate the surface characteristics, we also applied dip-coating process on glass slides by using the same process.

2.2.1 Preparation Before Dip-coating

The cotton fabric was ultrasonically cleaned with water, ethanol and toluene to remove possible impurities, and then dried in an oven at 60 ℃.

The glass fiber membranes were cleaned by immersion in piranha solution (3:1 mixture of 98% H_2SO_4 and 30% H_2O_2; piranha solutions may result in explosion or skin burns if not handled with extreme caution!) for 15 min. Afterwards, the substrates were thoroughly rinsed with DI water, and dried under nitrogen flow.

Polyester (PET) filters were treated in UV-Ozone for 30 min.

2.2.2 Dip-coating of HBO Polymer

The custom-designed HBO polymer was diluted with DI water to 10% of its stock concentration. Immerse the substrates (cotton fabrics, glass fibers, and polyester filters) into the diluted polymer solution for 1 hr. Afterwards, rinse the coated substrates in DI water several times. Then the substrates were dried by nitrogen flow first and then in over at 60 ℃ for 4 hrs or dried at room temperature for 24 hrs.

2.2.3 Dip-coating Process

The custom-designed OBH polymer was diluted with naphtha to 10% of its stock concentration. Immerse the substrates into the diluted polymer solution for 1 hr. Rinse the coated substrates in mineral spirit several times. Then the substrates were dried by nitrogen flow first and then in over at 60 ℃ for 4 hrs or dried at room temperature for 24 hrs.

The polyester (PET) filters were coated by the following steps, which are based on the "PET modification by end-capped fluoroalkyl-functional silanes method" (Kawase & Sawada, End-capped fluoroalkyl-functional silanes. Part II: Modification of polymers and possibility of multifunctional silanes, 2002). Dip-coating by 1% (TRIDECAFLUORO -1,1,2,2-TETRAHYDROOCTYL) TRICHLOROSILANE (a product of Gelest, Inc.) which is diluted by hexane. Then, PET is heated in an oven at 120 ℃, 5 min. After the heat treatment, PET was rinsed with pure hexane for 5 min with ultrasonic agitation. Then the substrates were dried in oven at 60 ℃ for 4 hours or dried in room temperature for 24 hours.

3.0 MEMBRANES CHARACTERIZATION METHOD

3.1 CONTACT ANGLE MEASUREMENT

The liquid contact angles were measured using a VCA-OPTIMA drop shape analysis system (AST Products, Inc.) with a computer-controlled liquid dispensing system. Liquid droplets in a volume of 2 μl were used to measure the static contact angle. All of the tests were performed under normal laboratory ambient conditions (20 ℃ and 40% relative humidity). Each contact angle measurement was repeated three times at different places of the sample, and the average value was reported.

3.2 VOLUME FLUX AND PRESSURE DROP CORRELATION MEASUREMENT

To measure the pressure drop as a function of the volume flux, formation of air bubbles in the fluid must be avoided. In the experiment, the separation tube was first kept vertical when the mixture was introduced into the tube and air was allowed to evacuate the tube while slowly rotating the tube until the tube was in a horizontal position and held by an iron support (shown in Figure 5).

3.3 BREAK-DOWN PRESSURE MEASUREMENT

The break-down pressure is measured by using a single component fluid (either water or oil) that the membrane is supposed to block, i.e. water for OBH membrane and oil (hexadecane) for HBO membrane. During the experiment, the single component fluid is continuously introduced into the tube and the pressure reading gradually increases. In a typical experiment, the reading of the pressure sensor goes up first and then drops abruptly when the liquid starts to penetrate the membrane. The highest reading is recorded as the break-down pressure.

As mentioned in the pressure drop measurement, the presence of air bubble may cause significant error in the pressure reading. Therefore, a relatively small flow rate is set for the pump. In the experiments, membrane area is about 373.25 mm^2, and a volumetric flow rate of 200 μL/min is used.

3.4 TIME DEPENDENCE OF MEMBRANE WETTABILITY

To determine whether the wettability of the membrane will vary as a function of time, the oil contact angle is measured as a function of time. Hexadecane, dodecane, octane, and hexane are used as oil component.

3.5 EXAMINATION OF WATER AND OIL CONTENT AFTER SEPARATION

3.5.1 Water Content in Separated Oil Stream

The method used in the measurement is developed based on American Society for Testing and Materials (ASTM) D4407 (Standard Test Method for Water Sediment in Crude Oil by the Centrifuge Method (Laboratory Procedure), Designation: D 4007–08).

This test method describes how water content in oil is determined by using a centrifuge procedure. The amount of water detected by this method is almost always lower than the actual water content. Although this method is not as accurate as the distillation method, it can still prove the effectiveness of OBH membrane if the water content result is low enough (say < 0.01 wt%).

The water sample to be tested is placed into a cone-shaped centrifuge tube. After centrifugation, the volume of water at the bottom of the tube is read.

3.5.2 Oil Content in Separated Water Stream

The method used in the measurement was developed based on ASTM standard D3921 (Standard Test Method for Oil and Grease and Petroleum Hydrocarbons in Water, Designation: D3921 – 96).

The original method was used to define the content of petroleum hydrocarbon in water and oil or grease in waste water based on infrared absorption. In this study, the oil component was hexadecane, which is one of the long chain alkane in crude oil. Therefore, the

method can be applied to determine the oil content in water after separation. The sampling and testing procedures are described below.

Mix the sample by shaking the original sample bottle. Check the pH of the liquid by touching pH-sensitive paper to the cap. If necessary, add sufficient sulfuric acid or sodium bisulfate to attain a pH of 2 or less.

The acidified sample of separated water is extracted serially with three 30-mL volumes of 1, 1, 2-trichloro-1, 2, 2-trifluoroethane (referred to in this test method as solvent). The extract is diluted to 100 mL and a portion is examined by infrared spectroscopy to measure the amount of oil and grease removed from the original sample. A major portion of the remaining extract is contacted with silica gel to remove polar substances, thereby providing a solution of hydrocarbons (in this case, only hexadecane). This treated extract is then similarly examined by infrared spectroscopy.

4.0 RESULT AND DISCUSSION

4.1 SURFACE CHARACTERISTICS

4.1.1 Contact Angle of Flat and Rough Surfaces

4.1.1.1 Flat Surfaces

Using the method mentioned in the previous Chapters (3.1), the wettability of each polymer-modified surface was investigated through contact angle measurement. After coating the plain glass slides with the custom-designed HBO polymer, the θ_{flat} values of water and hexadecane were measured to be ~ 18 °and 70 °, respectively (see Figure 6).

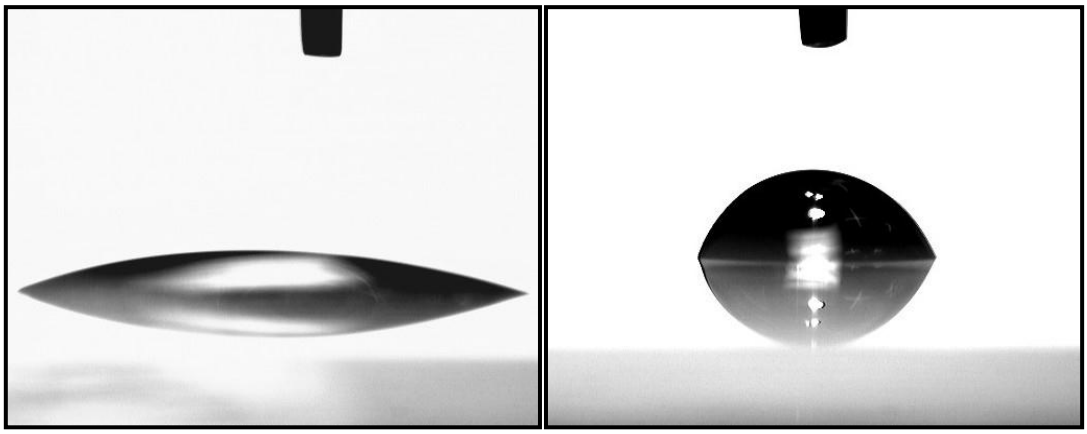

Figure 6 Contact angle of water and hexadecane on glass slide.

As introduced in Section 1.3.1, the θ_{flat} is the intrinsic contact angle defined as the contact angle on an ideally flat surface, which possesses the same surface chemistry as the textured surface. Apparently, here the intrinsic oil contact angle is much higher than the intrinsic water contact angle measured on the same surface, but both of them are less than 90 °.

4.1.1.2 Rough Surfaces

For the cotton fabric, after grafting the same HBO polymer as the glass slides, the textured surface exhibits a superhydrophilic but superoleophobic properties (Figure 7). In the graph, the blue stain is a droplet of dyed water which completely spreads out on (or is absorbed by) the cotton fabric surface; the transparent fluid is hexadecane which has a contact angle greater than 90 °.

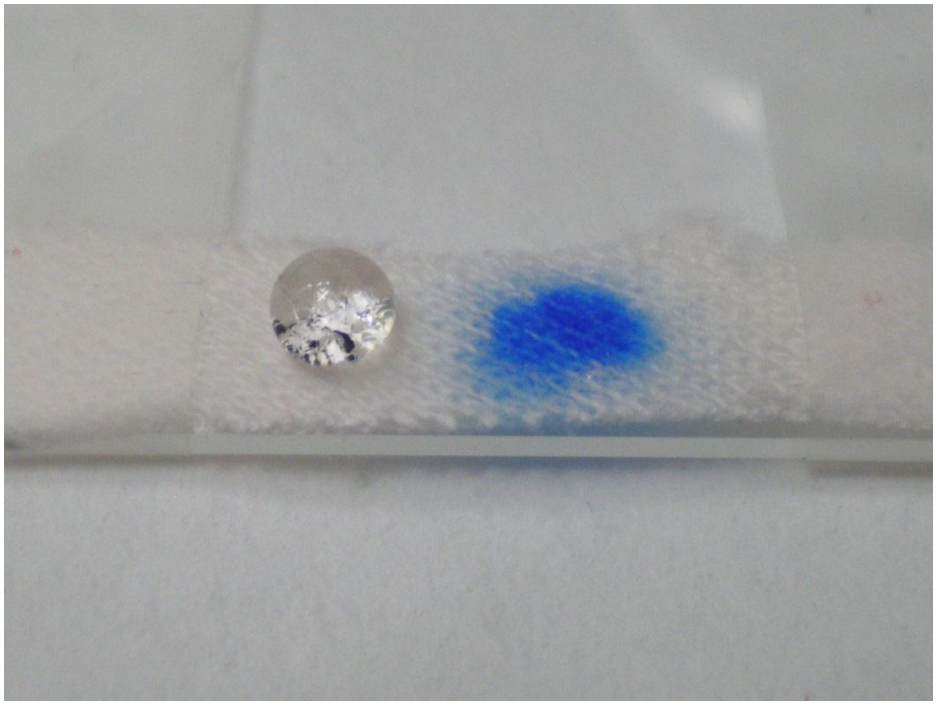

Figure 7 Optical image of hexadecane and water on HBO polymer-modified surface of cotton fabric.

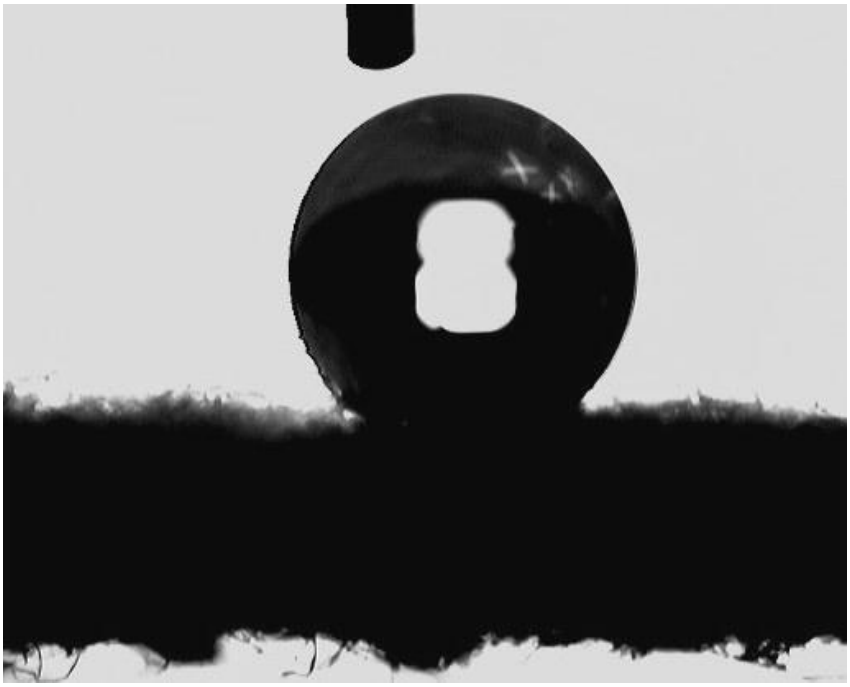

Figure 8 Contact angle measurement of hexadecane on HBO polymer-modified cotton fabric.

The hexadecane contact angle was measured to be above 150 ° (Figure 8) and the sliding angle was found to be less than 5 °. The water penetration process was recorded under contact angle measurement approach (Figure 9, from step A to step D).

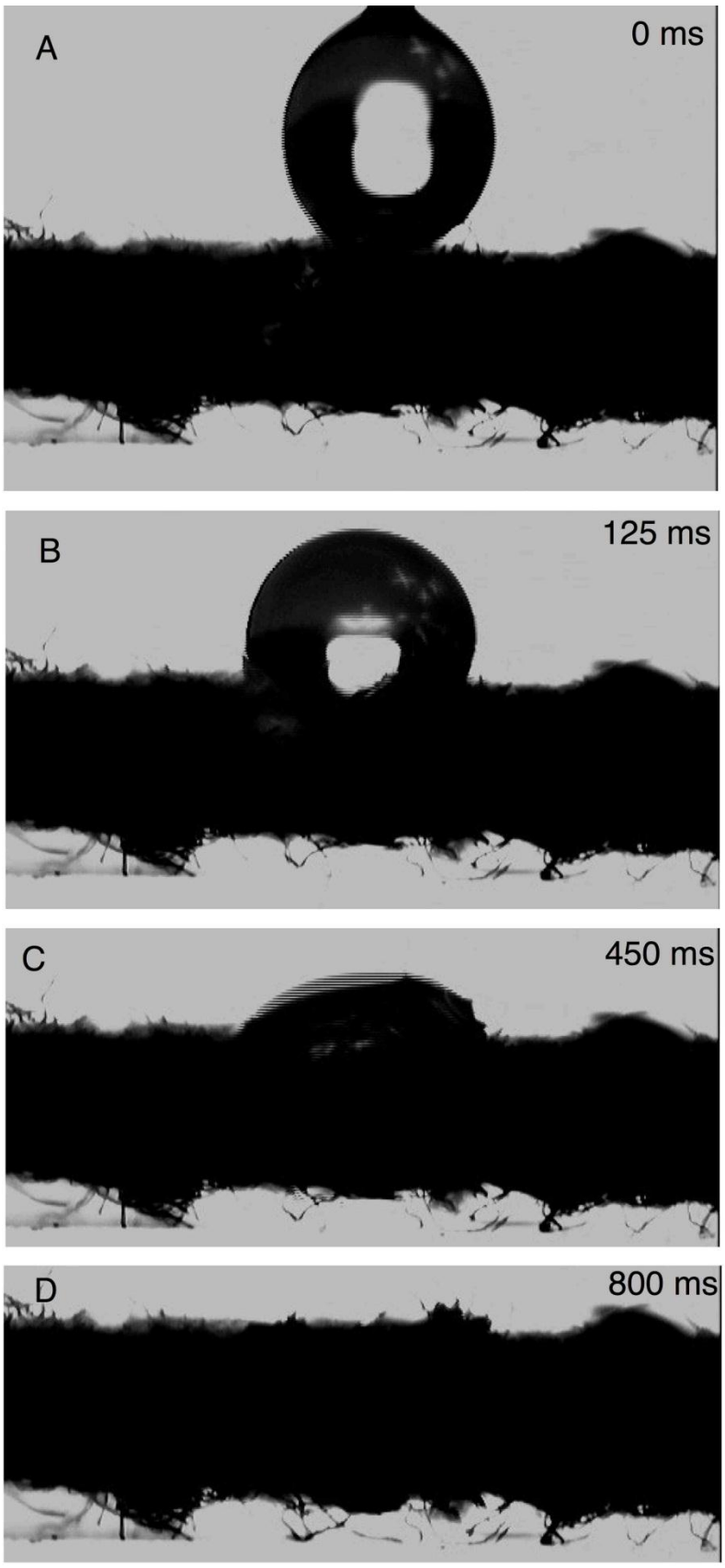

Figure 9 Water penetration process on HBO cotton fabric.

4.1.2 Discussion

The observed oil-repellency may be explained by metastable Cassie-Baxter model introduced in Chapter 1.4.2.

In the Cassie-Baxter state, the liquid droplet is thought to be in contact with a composite surface of solid and air, that is, air was trapped between solid and liquid phase (Figure 2, B). In this situation, even though $\theta_{flat} < 90°$, it is still possible for the surface to achieve super-hydro/oleo-phobic due to the trapped air pockets.

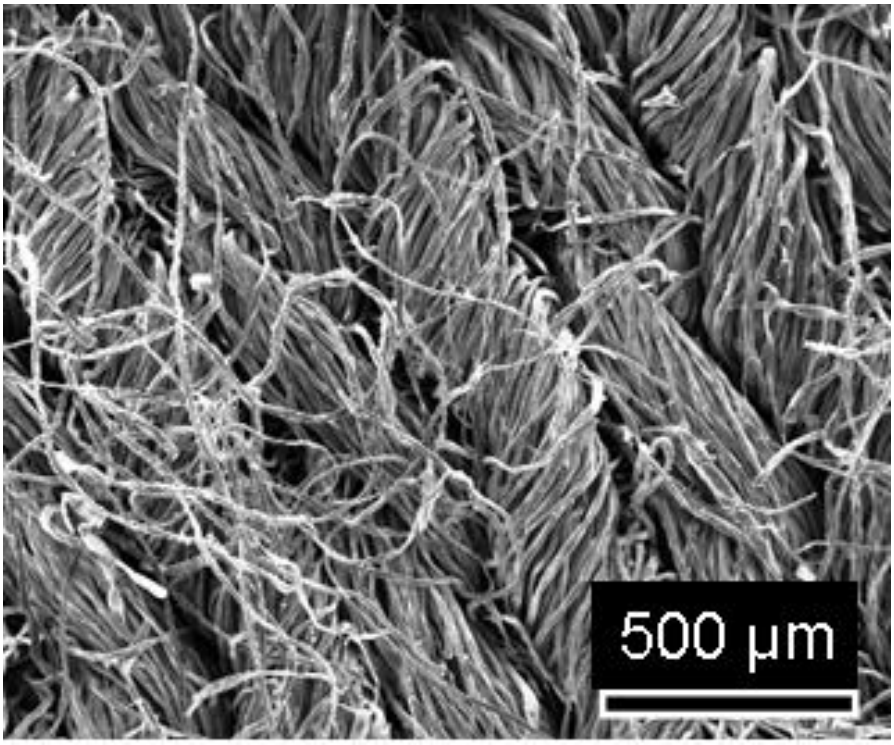

Figure 10 SEM image of cotton fabric structure.

SEM images displaying the representative surface morphology of the cotton fabric, glass fiber and polyester filter are shown in Figure 10, Figure 11, and Figure 12, respectively. It is clear that the individual fibers (here approximately treated as cylindrical features) may form the re-entrant texture as previously reported (see Figure 3). In addition, this structure is still maintaining its original appearance after coating with custom-designed polymer (see Figure 13). When a liquid is in contact with such surface texture, the capillary force may prevent the liquid from completely penetrating the pores of the surface texture once the local texture angle (ψ, ranging from 0 °to 180 °for the cylindrical features) is less than the θ_{flat}, even if the θ_{flat} of the liquid may be much smaller than 90 °.

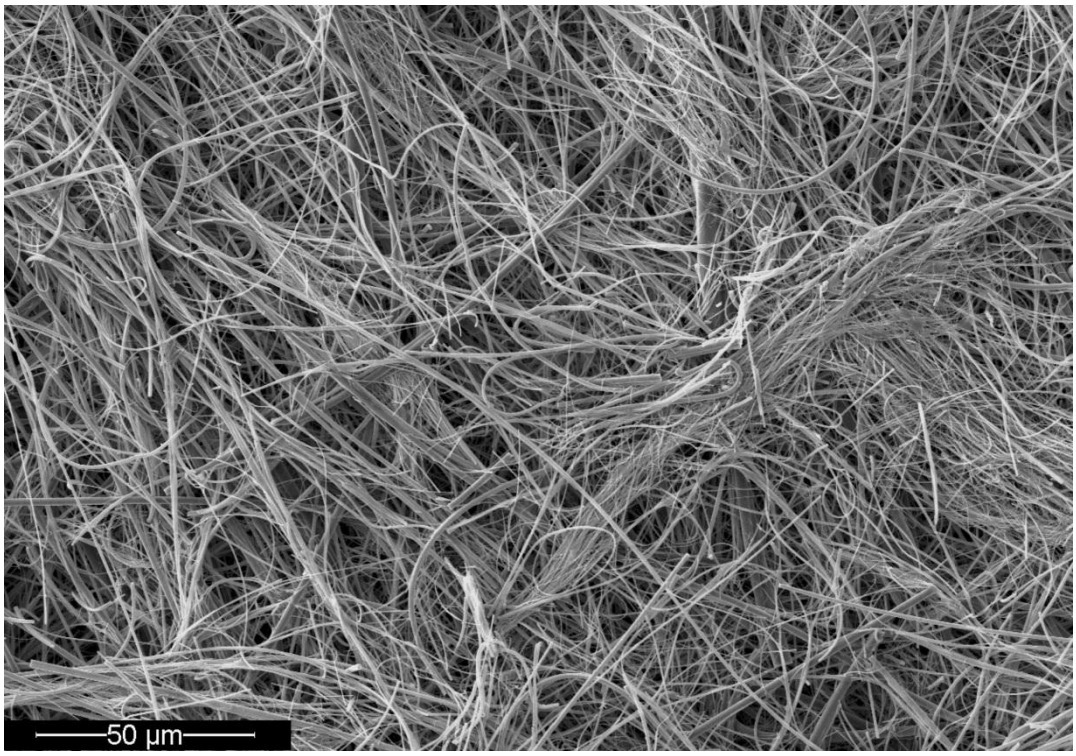

Figure 11 SEM image of glass fiber structure.

As a result, the formation of the metastable Cassie-Baxter state will enhance the surface repellency by introducing the air pockets underneath the liquid, and lead to a very high θ_{rough} or even a low contact angle hysteresis (defined as the difference between the advancing and receding contact angles). This explanation may help us understand the observed superoleophobic behavior on the treated fabrics, with a relatively low θ_{flat} of ~70 °but a very high θ_{rough} of above 150 °for hexadecane.

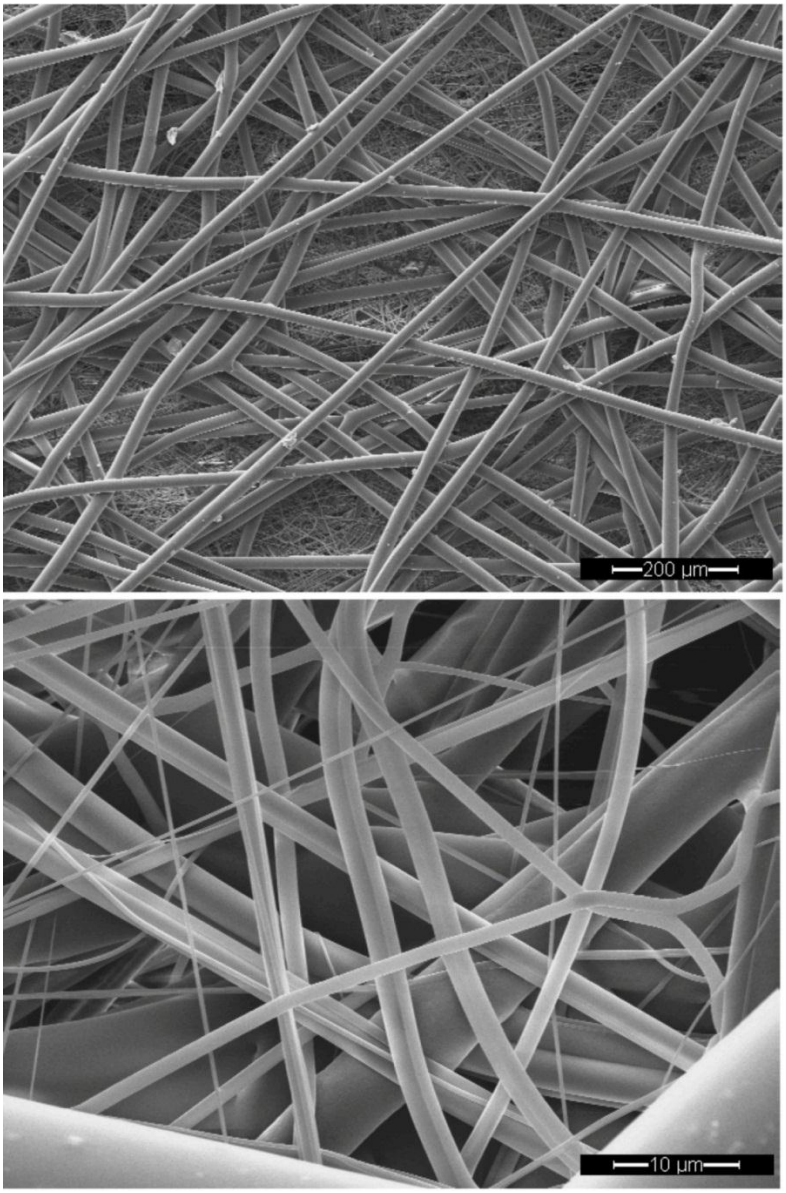

Figure 12 SEM image of polyester filter structure.

For water with a θ_{flat} of ~18°, a fragile Cassie-Baxter state can also be perceived (Figure 9, Step A and B), which transiently collapses and has an extremely short lifetime of less than 0.5 s (~ 450 ms). Afterwards, water spreads quickly and is totally imbibed by the fabric within 350 ms. During this process, the Cassie-Baxter state is switched to the Wenzel state, where the surface roughness amplifies the wetting behavior of the intrinsically hydrophilic material ($\theta_{flat} \approx 18°$) and leads to the complete wetting.

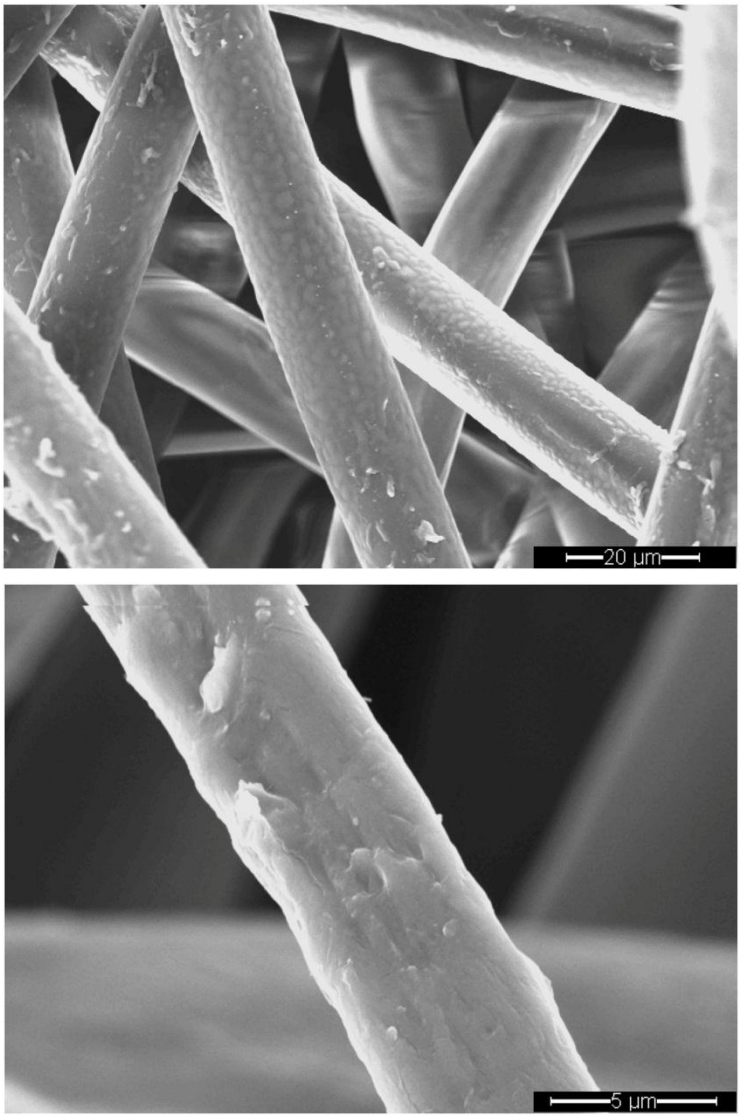

Figure 13 SEM image of coated glass fiber membrane.

4.1.3 Robustness Evaluation

As introduced in Section 1.4.2, two robustness factors, the robustness height (H*) and the robustness angle (T*) are used to evaluate the robustness of the polymer-modified membranes. Through increasing the magnitude of the robustness parameters (H* and T*), the stability of the metastable composite interface can be enhanced.

The parameter H*, arising from the ratio of the sagging height (h_1) and the maximum pore depth (h_2) (see Figure 3), is given as

$$H^* = (1-\cos\theta)R\ell_{cap}/D^2 \tag{4.1}$$

where R is the fiber radius, $\ell_{cap} = \sqrt{\gamma_{lv}/\rho g}$ is the capillary length of the liquid, γ_{lv} is the liquid surface tension, ρ is the liquid density, g is the acceleration due to gravity, and D is the half of the inter-fiber gap.

The parameter T*, arising from the sagging angle of $\delta\theta = \theta - \psi_{\min}$, is given as

$$T^* = \ell_{cap}\sin(\theta - \psi_{\min})/(2D) \tag{4.2}$$

and the minimum local texture angle $\psi_{\min}$ used herein equals to 0.

For a fixed solid material, it is clear that the robustness parameters are determined by two independent factors: the liquid properties (θ and ℓ_{cap}) and the surface properties (R, D and $\psi_{\min}$).

4.1.3.1 HBO Polymer-modified Surface

In this section, the robustness of superhydrophilic but superhydrophobic surfaces (take cotton fabric as an example to present the data) modified by HBO polymer were evaluated.

On the cotton fabric surface (see Figure 10), a two-tier hierarchical structure, consisting of individual fibers and fiber bundles, is observed, which makes it difficult to quantitatively determine the robustness parameters. Therefore, the robustness factors have been modified and interpreted in relative form.

The following compares the robustness of the Cassie-Baxter state of two liquids, namely water and hexadecane, on a surface. With the same surface texture, the surface topography parameters (R , D and $\psi_{\min}$) are fixed and are not functions of the test liquids. Therefore, the relative robustness parameters of liquid can be expressed as the following:

Relative robustness height

$$RH^* = \frac{H^*_{liquid}}{H^*_{reference}} = \left(\frac{1-\cos\theta_{liquid}}{1-\cos\theta_{reference}} \right) \left(\sqrt{\frac{\gamma_{lv,liquid}\rho_{reference}}{\gamma_{lv,reference}\rho_{liquid}}} \right) \tag{4.3}$$

Relative robustness angle

$$RT^* = \frac{T^*_{liquid}}{T^*_{reference}} = \frac{\sin(\theta_{liquid}-\psi_{\min})}{\sin(\theta_{reference}-\psi_{\min})} \left(\sqrt{\frac{\gamma_{lv,liquid}\rho_{reference}}{\gamma_{lv,reference}\rho_{liquid}}} \right) \tag{4.4}$$

Water has been chosen as the reference liquid, with $\theta_{water} = 18°$, $\gamma_{lv,water} = 72.1\ \text{mN/m}$, and $\rho_{water} = 1000\ \text{kg/m}^3$. Relative robustness parameters for hexadecane, with $\theta_{hexadecane} = 70°$, $\gamma_{lv,hexadecane} = 27.5\ \text{mN/m}$, and $\rho_{hexadecane} = 773\ \text{kg/m}^3$, are calculated comparing to water.

RH^* was calculated to be ~ 9.5 and RT^* to be ~2.1, which indicate that hexadecane may maintain a much more robust Cassie-Baxter state than water. The result obtained from this analysis provides a quantitative explanation to the observed superoleophobic but superhydrophilic phenomena.

4.2 BREAK-DOWN PRESSURE

As mentioned in Section 3.3, based on the robustness analysis in Section 4.1.3, the break-down pressure can be redefined as the pressure that drives liquid sagging height h_1 (in Figure 3) to be higher than the product of robustness height and maximum pore depth $h_2 \bullet H^*$. For the same surface texture, the surface geological parameters (R, D and $\psi_{\min}$) are fixed, so the robustness parameters for certain liquid are fixed as well. Since break-down pressure determines the operational pressure range of a membrane, measuring the break-down pressure is of great importance to the design of water-oil separators. Break-down pressures of several membranes were measured and the results are listed in Table 2.

Table 2 Break-down Pressure (Pa) of Water-pass (HBO) and Oil-pass (OBH) Membranes

Membrane Type	Cotton Fabric	Ceramic Filter	Glass Filter #1	Glass Filter #2	Glass Filter #3	PET Membrane
Water-pass (HBO)	495.43	N/A	7844.4	7555.4	7761.8	454.15
Oil-pass (OBH)	578	578	10156.4	9165.6	12881.3	2064.3

Note:

Glass Filter #1: pore 1.0μm, thickness 660 μm
Glass Filter #2: pore 1.0μm, thickness 330 μm
Glass Filter #3: pore 0.5μm, thickness 330 μm

4.3 VOLUME FLUX AND PRESSURE CORRELATION

Flow rate (mL/min) is measured and recorded in terms of pressure. However, in the later Chapter (5.0), the curve of volume flux vs. pressure is used to design the continuous separator, flow rate vs. pressure plot will show the same trend if the membrane area is fixed.

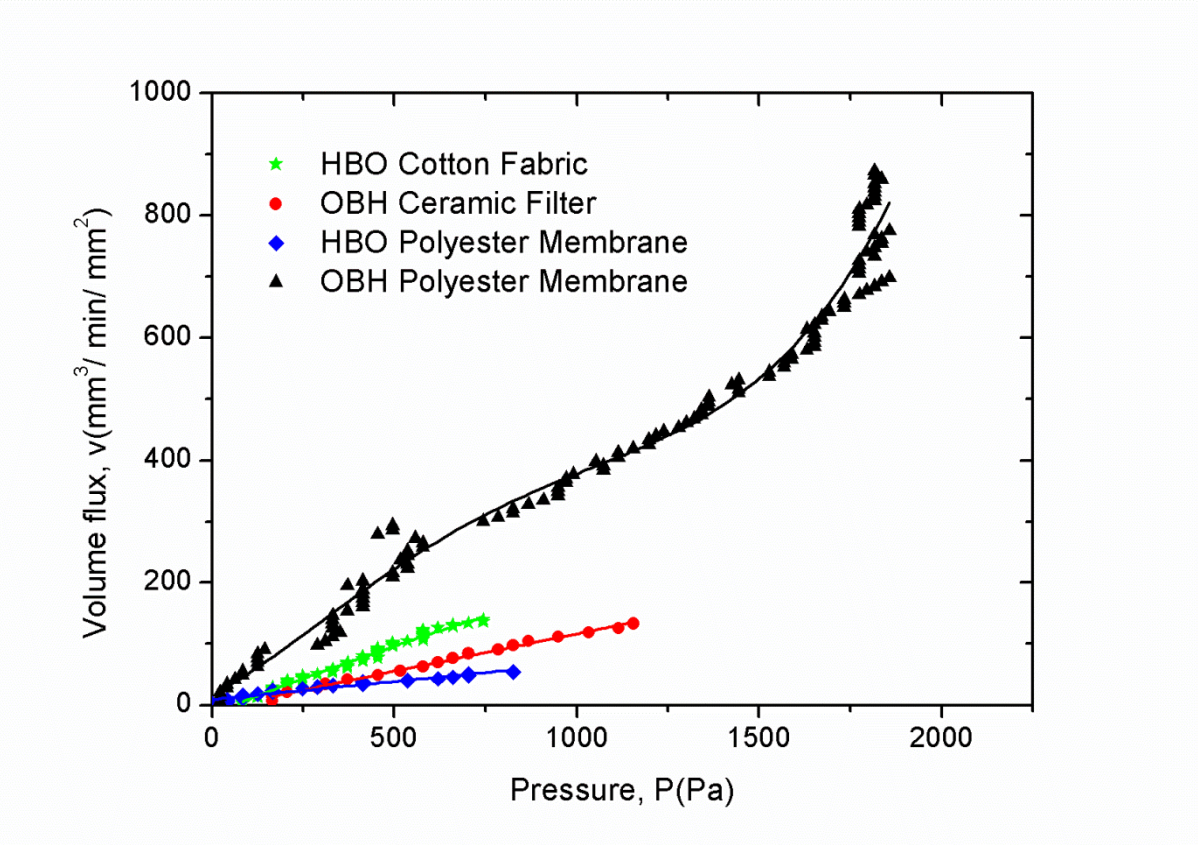

Figure 14 Volume flux ($mm^3/min/mm^2$) in terms of pressure curve of HBO cotton fabric, HBO polyester (PET) filter, OBH ceramic filter, and OBH polyester (PET) filter.

Figure 14 plots the volume flux as a function of pressure drop for four different membranes. For a typical membrane, the pressure drop should increase with volume flux with a behavior between first and second order (Tarabara, Hovinga, & Wiesner, 2002). After fitting the data points shown in Figure 14, the order of fitting curve ranges from 1.0 to 1.3 which agrees with normal membranes behaviors.

4.4 TIME DEPENDENCE OF MEMBRANE WETTABILITY

4.4.1 Time Dependence of Contact Angle

The hexadecane, dodecane, octane contact angle on the HBO membrane decreases with time. The time for contact angle to drop below 90^{o} is 100 hrs, 35 mins, and 1min, respectively (see Figure 15, 16, and 17).

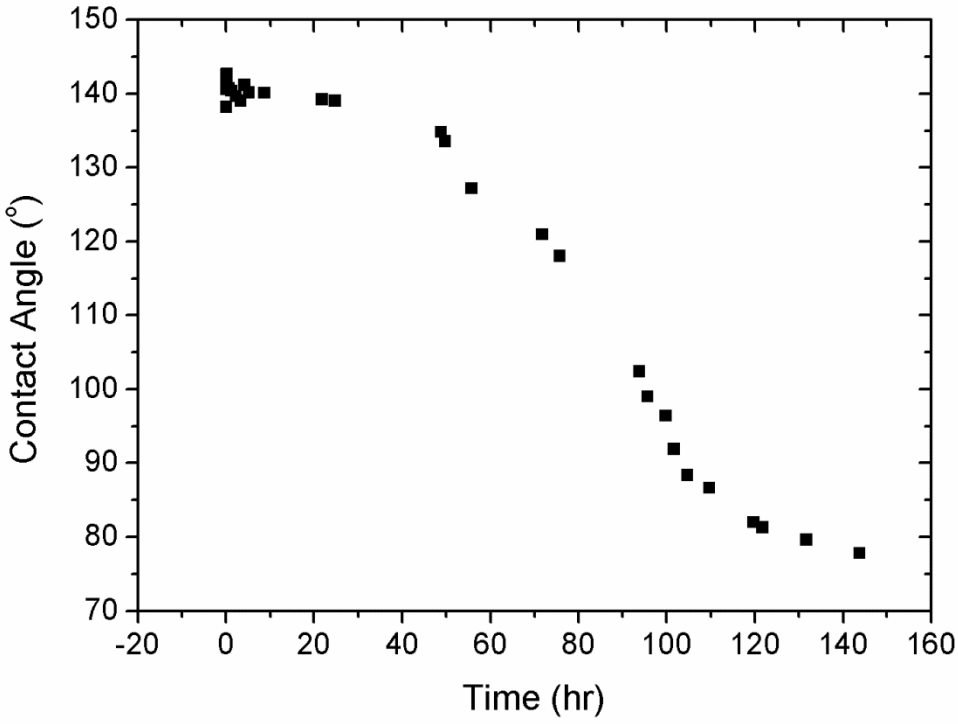

Figure 15 Hexadecane contact angle on HBO membrane as a function of time.

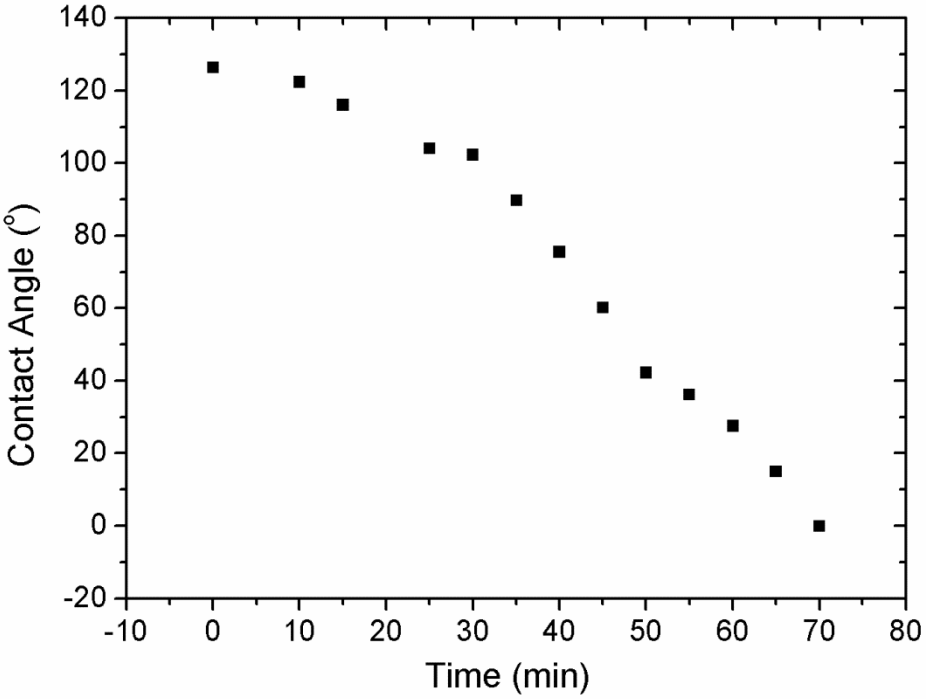

Figure 16 Dodecane contact angle on HBO membrane as a function of time.

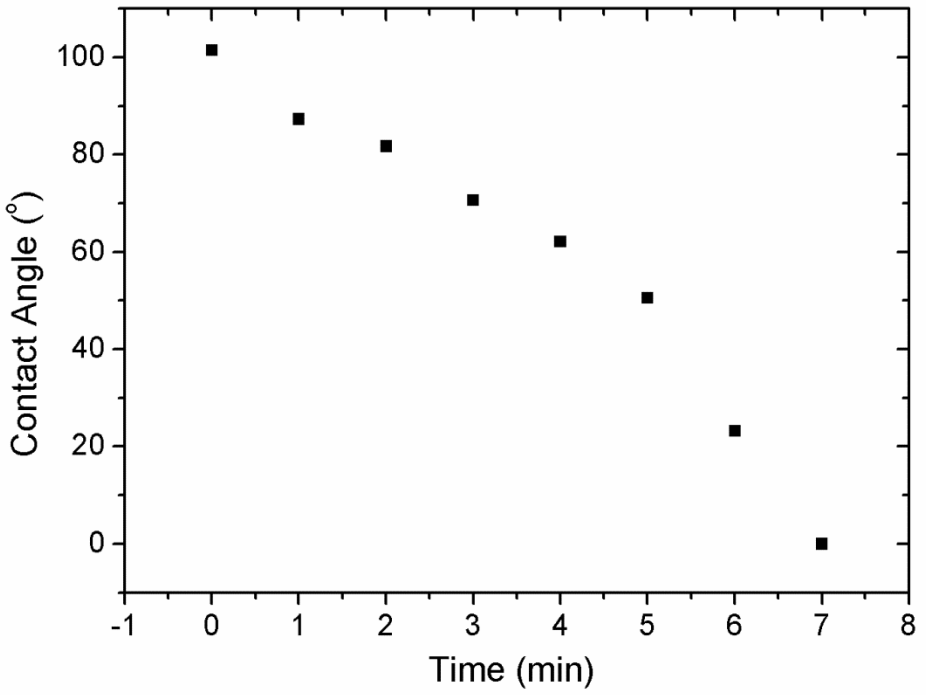

Figure 17 Octane contact angle on HBO membrane as a function of time.

5.0 DESIGN AND FABRICATION OF A CONTINUOUS WATER-OIL SEPARATOR

As shown in Figure 4 and Figure 5, the device is set up for both the 'volume flux vs. pressure' test and the 'break-down pressure' test. One end of a small-diameter hose connecting with a pressure sensor is placed in the center of the cylindrical separation tube and close to the separation membrane.

The pressure sensor (Omega PX26-001GV) has a measuring range of 0-1 psi (0-6894.75729 Pa). Another pressure sensor (Omega PX26-001GV) was used when the break-down pressure of glass fibers have exceeded the measuring range of the first pressure sensor. The second pressure sensor used here has a measuring range of 0-5 psi (0-34473.78645 Pa).

Voltage source of the pressure sensor is provided by KELTHLEY Model 6487 Voltage Source. Voltage drop was measured by KELTHLEY Model 2400 Measure Meter. Flow rate is controlled by a syringe pump (PHD 2000 Syringe Pump, Instech Laboratories, Inc.). Syringes (Syringes HSW NORM-JECT, 50 ml (60 ml)) are purchased from Henke-Sass,WolfGmbH.

A membrane with a high break-down pressure and a relatively high volume flux ($mm^3/min/mm^2$) is preferable. Although glass fibers have a dramatically high break-down pressure, the volume flux is much lower than other membranes. In addition, due to the

unstable internal structure of the three glass fibers used here, they often break apart mechanically during the water-oil separation process. Therefore, we used HBO cotton fabric and OBH polyester (PET) filters in our separator. The volume flux as a function of pressure drop for the HBO cotton fabric and OBH PET membrane is shown in Figure 18.

The operating pressure needs to be chosen within the effective pressure range. In this case, 454 Pa is an appropriate operating pressure. Based on Figure 18, we can determine the volume flux of each membrane under the operating pressure. The surface areas of the separation membranes can be determined by using equation (5.1), (5.2) and (5.3)

$$Q_w / Q_o = V_w / V_o \tag{5.1}$$

$$Q_w = F_w A_w \tag{5.2}$$

$$Q_o = F_o A_o \tag{5.3}$$

Note:

V_w = volume of water in the mixture [mm^3]
V_o = volume of oil in the mixture [mm^3]
Q_w = volume flow rate of water [mm^3/min]
Q_o = volume flow rate of oil [mm^3/min]
F_w = volume flux of water [mm^3/min/mm^2]
F_o = volume flux of oil [mm^3/min/mm^2]
A_w = area of water-pass membrane [mm^2]
A_o = area of oil-pass membrane [mm^2]

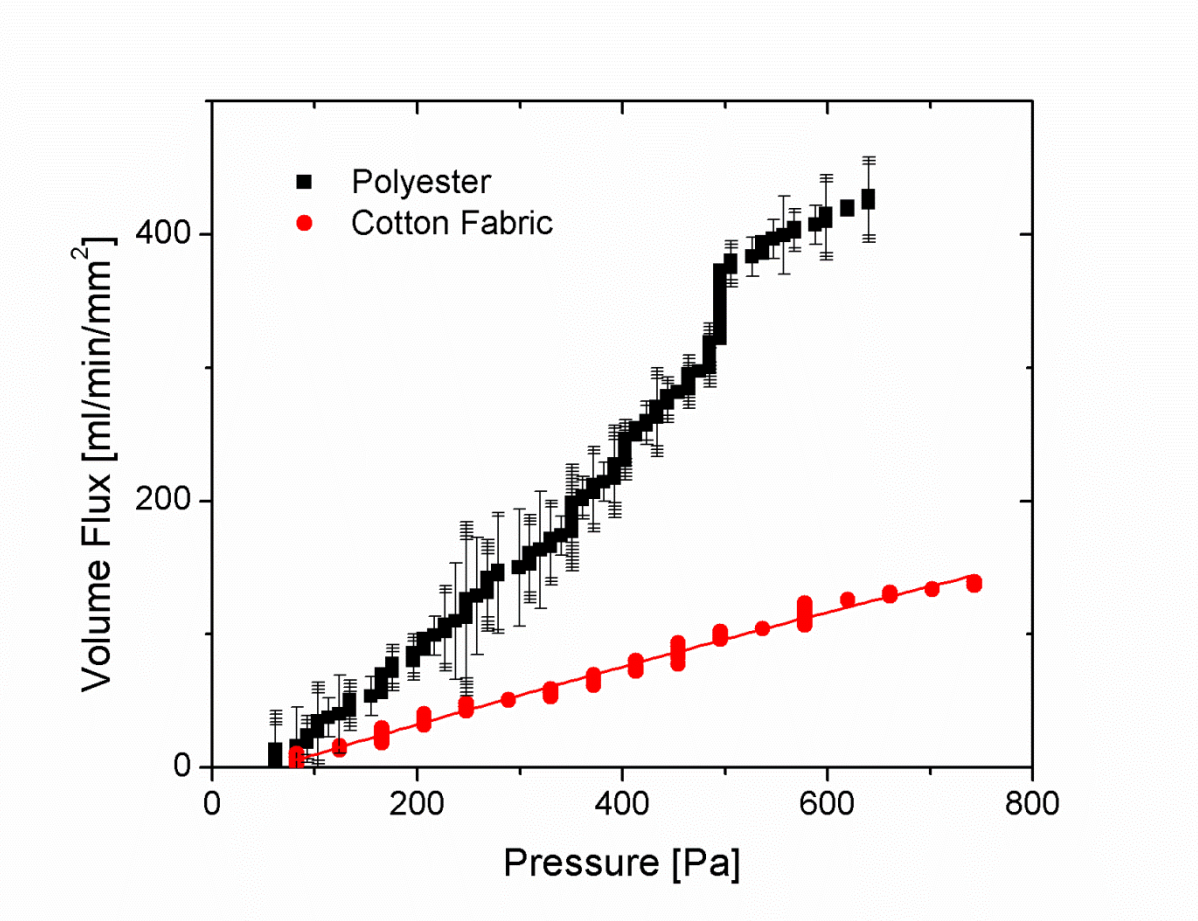

Figure 18 Volume flux in terms of pressure curve of HBO cotton fabric and OBH polyester (PET) filter.

At operating pressure of 454 Pa, the volume flux of oil-pass PET membrane and water-pass cotton fabric are 281.31 and 93.77 $mm^3/min/mm^2$, respectively. Therefore, in order to separate 1:1 water-oil mixture, the areas of the oil-pass PET membrane and water-pass cotton fabric are 124.4 and 373.3 mm^2, respectively. The processing capability of this separator is estimated to be about 4.2 liter of water-oil mixture (1:1) per hour (under the assumed operating point pressure 454 Pa).

6.0 SUMMARY

This thesis consists of three major parts of research work.

First, a surface modification process is developed to coat several membrane substrates, including cotton fabrics, ceramic filters, polyester (PET) filters, and glass fiber membranes, with custom-designed polymers. After the surface modification, these membranes can be made either “superhydrophilic but superoleophobic (referred as HBO)” or “superoleophilic but superhydrophobic (refered as OBH)”.

Second, the morphology and wettability of the surface modified membranes are characterized. The HBO and OBH phenomena are explained by using the Cassie-Baxter model and analyzed by introducing the robustness height H* and robustness angle T*, which are critical parameters to characterize the stability of the Cassie-Baxter state. The relative robustness height RH* and relative robustness angle RT* are determined for oil and water on a specific substrate.

Third, separation performance of membranes is characterized by measuring break-down pressure and volume flux – pressure drop relationship. Based on these data, a lab-scale continunous water-oil separator is designed and fabricated, which is able to separate 4.2 liter of water-oil mixture (at a volume ratio of 1:1) per hour. Methods adopted from ASTM are used to measure the oil and water content in the effluent flows. The result shows

that the oil content in the separated water stream is less than the minimum detectable value of 0.075 wt%, and water content in the separated oil stream is less than the detectable value of 0.01 wt%.

BIBLIOGRAPHY

Belaidi, A., & Thew, M. (2003). The Effect of Oil and Gas Content on the Controllability and Separation in a De-Oiling Hydrocyclone. *Chemical Engineering Research and Design, 81*(3), 305-314.

Boreyko, J. B., Baker, C. H., Poley, C. R., & Chen, C. (2011). Wetting and dewetting transitions on hierarchical superhydrophobic surfaces. *Langmuir, 27*, 7502–7509.

Cao, L. (2010). Superhydrophobic surface: Design, fabrication, and applications. *Dissertation*, University of Pittsburgh.

Cao, L. (2010). Superhydrophobic surface: Design, fabrication, and applications. *Dissertation*, University of Pittsburgh.

Cao, L., Hu, H., & Gao, D. (2007). Design and Fabrication of Micro-textures for Inducing a Superhydrophobic Behavior on Hydrophilic Materials. *Langmuir, 23*, 4310-4314.

Cassie, A., & Baxter, S. (1944). Wettability of porous surfaces. *Trans. Faraday Soc., 40*, 546-551.

Standard Test Method for Water Sediment in Crude Oil by the Centrifuge Method (Laboratory Procedure). (Designation: D 4007–08). *Manual of Petroleum Measurement Standards (MPMS)*, Chapter 10.3.

Standard Test Method for Water Sediment in Crude Oil by the Centrifuge Method (Laboratory Procedure). (Designation: D 4007–08). *Manual of Petroleum Measurement Standards (MPMS)*, Chapter 10.3.

Standard Test Method for Oil and Grease and Petroleum Hydrocarbons in Water. (Designation: D3921 – 96). *Manual of Petroleum Measurement Standards (MPMS)*.

Standard Test Method for Oil and Grease and Petroleum Hydrocarbons in Water. (Designation: D3921 – 96). *Manual of Petroleum Measurement Standards (MPMS)*.

Fernandez, L., Soria, C., Garcia-Tourn, & Izquierdo, M. (2001). The study of Oil/Water Separation in Emulsion by Membrane Technology. *SPE Latin American and Caribbean Petroleum Engineering Conference.* Buenos Aires, Argentina.

Howarter, J., & Youngblood, J. (2007). Self-cleaning and anti-fog surfaces via stimuli-responsive polymer brushes. *Advanced Materials, 19*(22), 3838.

Kawase, T., & Sawada, H. (2002). End-capped fluoroalkyl-functional silanes. Part II: Modification of polymers and possibility of multifunctional silanes. *J. Adhesion Sci. Technol, 16*, 1121-1140.

Kawase, T., & Sawada, H. (2002). End-capped fluoroalkyl-functional silanes. Part II: Modification of polymers and possibility of multifunctional silanes. *J. Adhesion Sci. Technol, 16*, 1121-1140.

Koishi, T., Yasuoka, K., Fujikawa, S., Ebisuzaki, T., & Zeng, X. (2009). Coexistence and transition between Cassie and Wenzel state on pillared hydrophobic surface. *PNAS, 106*(21), 8435-8440.

Oshida, Y., Sachdeva, R., & Miyazaki, S. (1992). Changes in contact angles as a function of time on some pre-oxidized biomaterials. *Journal of Materials Science: Materials in Medicine, 3*(4), 306-312.

Rao, T., & Patil, D. (1998). Developments in gravity separation. *Journal of Mines, Metals and Fuels, 46*(11), 383-388.

Tarabara, V., Hovinga, R., & Wiesner, M. (2002). Constant Transmembrane Pressure vs. Constant Permeate Flux: Effect of Particle Size on Crossflow Membrane Filtration. *Environ Eng Sci, 19*(6), 343-355.

Taylor, S. (1996). Theory and practice of electrically-enhanced phase separation of water-in-oil emulsions. *Chemical Engineering Research and Design, 74*(5), 526-540.

Tuteja, A., Choi, W., Ma, M., Mabry, J., Mazzella, S., Rutledge, G., et al. (2007). Designing Superoleophobic Surfaces. *Science, 318*(5856), 1618.

Tuteja, A., Choi, W., Mabry, J., McKinley, G., & Cohen, R. (2008). Robust omniphobic surfaces. *Proc. Natl. Acad. Sci., 105*(47), 18200-18205.

Tuteja, A., Choi, W., Mabry, J., McKinley, G., & Cohen, R. (2008). Robust omniphobic surfaces. *Proc. Natl. Acad. Sci., 105*(47), 18200-18205.

Tuteja, A., Choi, W., McKinley, G., Cohen, R., & Rubner, M. (2008). Design Parameters for Superhydrophobicity and Superoleophobicity. *MRS Bulletin, 33*, 752-758.

Varanasi, K. K., Deng, T., Hsu, M., & Bhate, N. (2009). Wetting hysteresis, metastability, and droplet impact on superhydrophobic surfaces. *Proceedings of the ASME InterPack Conference* (pp. 623-630). San Francisco, Calif, USA: IPACK '09.

Wenzel, R. (1936). Resistance of solid surfaces to wetting by water. *Ind. Eng. Chem., 28*, 988-994.

Wenzel, R. (1936). Resistance of solid surfaces to wetting by water. *Ind. Eng. Chem., 28*, 988-994.

Wenzel, R. (1936). Resistance of solid surfaces to wetting by water. *Ind. Eng. Chem., 28*, 988-994.

Young, T. (1805). An essay on the cohesion of fluids. *Philos. Trans. R. Soc., 95*, 65.